A theoretical model for the orientation of carbene insertion into saturated hydrocarbons and the origin of the activation barrier

ARTICLE *in* JOURNAL OF THE AMERICAN CHEMICAL SOCIETY · NOVEMBER 1993

Impact Factor: 12.11 · DOI: 10.1021/ja00075a045

5 AUTHORS, INCLUDING:

Robert D. Bach
University of Delaware
198 PUBLICATIONS **4,975** CITATIONS

A Theoretical Model for the Orientation of Carbene Insertion into Saturated Hydrocarbons and the Origin of the Activation Barrier

Robert D. Bach,* Ming-Der Su, Ehab Aldabbagh, Jose L. Andrés,† and H. Bernhard Schlegel

Contribution from the Department of Chemistry, Wayne State University, Detroit, Michigan 48202

Received March 17, 1993®

Abstract: Transition states for carbene insertion reactions into C–H bonds can be classified as σ or π approaches. In the π approach, the empty orbital of the carbene is aligned with the carbon p orbital of the π_{CH2} fragment orbital; in the σ approach, the empty carbene p orbital is aligned with the σ_{CH2} fragment orbital. Concerted hydrogen migration to the larger lobe of the carbene lone pair is energetically favorable. The transition state for CH_2 insertion into methane has been calculated at the HF/6-31G*, MP2/6-31G*, and QCISD/6-31G* levels. At all levels, the σ approach is slightly favored over the π approach. The barrier at HF is too high, and the C–C bond in the transition state is too short. A small barrier (0.4 kcal/mol) relative to a long-range complex was found at the QCISD/6-31G* level, but none is found at QCISD(T)/6-31G* and QCISD/6-311G**. Transition states have also been optimized at the HF/6-31G* and MP2/6-31G* levels for $HCCH_3$, $C(CH_3)_2$, CHF, and CF_2 inserting into methane. The σ approach is again slightly favored over π. For vinylidene ($C{=}CH_2$) there is a slight preference for the π approach for insertion into both methane and ethane. Transition states for insertion of CH_2, $HCCH_3$, $C(CH_3)_2$, CF_2, vinylidene, and silylene into ethane have been optimized at HF/6-31G* and MP2/6-31G*. The σ_{CH2} pathways are favored over π_{CH2} and π_{CHCH3} with σ_{CHCH3} lying significantly higher. For the carbenes considered, there is a wide variation in the barrier heights. The transition state with the carbene in an inverted orientation and the hydrogen migrating to the wrong side of the carbene lone pair is typically 5–10 kcal/mol higher. Contrary to expectations, the barrier heights do not correlate with the HOMO or LUMO energies or the HOMO–LUMO gap. Instead, the trend correlates with the singlet–triplet energy differences in the carbenes. The valence bond state correlation method has been used to develop an explanation for the barrier heights.

Introduction

Traditionally, descriptive organic chemistry and the reactivity of organic compounds have been organized by functional groups. Until recently, saturated hydrocarbons, as a class of organic chemicals, have been conspicuously absent from discussions of closed-shell reactions.[1] The observation of facile oxygen insertion into the C–H bonds in transition metal mediated biochemical processes[2] and newly developed chemical reagents with a high propensity for oxygen donation (e.g. dioxiranes)[3] stands in stark contrast to the expectations initially held for this class of "unreactive" organic substrates. A mechanistic rationale for the concerted insertion of carbon, oxygen, and metal atoms into the σ bonds of saturated hydrocarbons remains a goal of mechanistic organic chemists.

We have recently described a frontier molecular orbital (FMO) model, based upon a set of fragment hydrocarbon molecular orbitals, that provides a rationale for the orientation of attack of an electrophilic species involved in the direct functionalization of saturated hydrocarbons.[4] As exemplified by **1**, we defined the electrophilic reagent E as having an electron deficient molecular orbital, capable of interacting with a doubly occupied hydrocarbon fragment orbital, and one or more pairs of electrons that may serve as the migration terminus for a 1,2-hydrogen shift. In a tetrahedral array both hydrogens bound to the sp^3 carbon of a methylene group (CH_2) occupy a common plane, and they are related by symmetry and are associated with an orbital with π symmetry (π_{CH2}) as in **2a** and a σ_{CH2} orbital as in **2b**.[5] Replacement of one of the hydrogens in a π_{CH2} fragment orbital by an alkyl group (e.g. CH_3) gives rise to a π_{CHCH3} fragment orbital (**2c**). In this FMO model we prefer to use canonical Hartree–Fock orbitals **2a**–**2c** and the σ/π nomenclature to describe the hydrocarbon fragment because it is easier to visualize the reaction trajectory and define the axis of attack of the electrophilic orbital on E (**1**). The localized description of the C–H σ bond is equally valid but very much harder to reconcile with the calculated geometries obtained for the transition states.

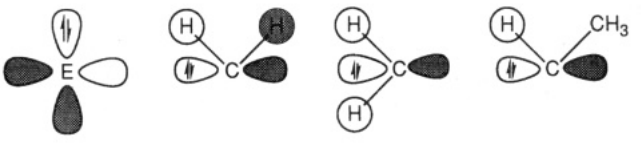

1 2a 2b 2c

In this study we describe the mechanism for insertion of singlet divalent carbon (CX_2, X = H, $=CH_2$, CH_3, F) and silicon (SiH_2) into saturated hydrocarbons. These electrophilic species typify

† Departament de Quimica, Universitat Autonoma de Barcelona, 08193 Bellaterra, Catalonia, Spain.

® Abstract published in *Advance ACS Abstracts,* October 1, 1993.

(1) (a) *Activation and Functionalization of Alkanes*; Hill, C. L., Ed.; John Wiley and Sons: New York, 1989. (b) Crabtree, R. H. *Chem. Rev.* **1985**, *85*, 245. (c) Janowicz, A. H.; Berman, R. G. *J. Am. Chem. Soc.* **1983**, *105*, 3929. Stoutland, P. O.; Bergman, R. G. *Ibid* **1988**, *110*, 5732. (d) Hoyano, J. K.; McMaster, A. D.; Grahman, W. A. E., *J. Am. Chem. Soc.* **1983**, *105*, 7190.

(2) (a) *Cytochrome P-450*; Montellano, P. R., Ed.; Plenum Press: New York, 1986. Ingold, K. U. *Aldrichimica Acta* **1989**, *22*, 69.

(3) (a) Murray, R. W. *Chem. Rev.* **1989**, *89*, 1187. (b) Adam, W.; Curci, R.; Edwards, J. O. *Acc. Chem. Soc.* **1989**, *22*, 205. (c) Murray, R. W.; Jeyareman, R.; Mohan, L. *J. Am. Chem. Soc.* **1986**, *108*, 2476. (d) Mello, R.; Rlorention, M.; Fusco, C.; Curci, R. *J. Am. Chem. Soc.* **1989**, *111*, 6749. (e) Adam, W.; Asensio, G.; Curci, R.; Gonzalez-Nunez, M. E.; Mello, R. *J. Org. Chem.* **1992**, *57*, 953. (f) Mello, R.; Cassidei, L.; Fiorentino, M.; Fusco, C.; Hümmer, W.; Jäger, V.; Curci, R. *J. Am. Chem. Soc.* **1991**, *113*, 2205.

(4) Bach, R. D.; Andres, J. L.; Owensby, A. L.; Su, M.-D.; McDouall, J. J. W. *J. Am. Chem. Soc.* **1993**, *115*, 5768.

(5) (a) For a discussion, see: Jorgensen, W. L.; Salem, L. *The Organic chemist's Book of Orbitals*; Academic Press: New York, 1973. (b) Meredith, C.; Hamilton, T. P.; Schaefer, H. F., III. *J. Phys. chem.* **1992**, *96*, 9250.

0002-7863/93/1515-10237$04.00/0

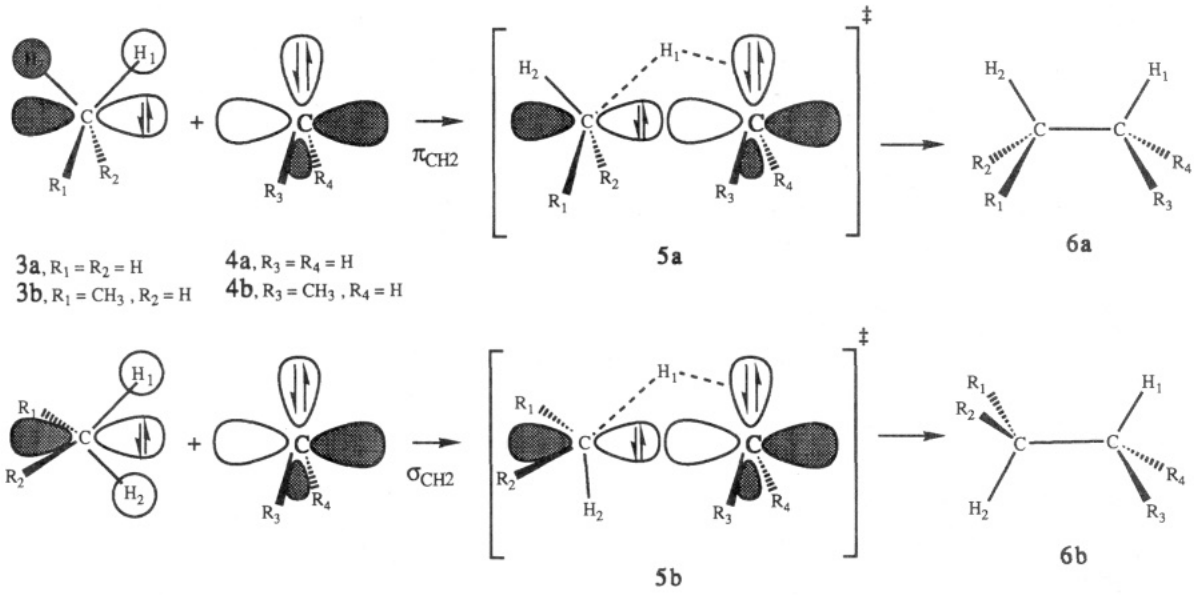

Figure 1. The insertion of carbenes into hydrocarbons can proceed along a π_{CH2} path, where the empty carbene p orbital is aligned with the carbon p orbital of a π_{CH2} fragment orbital, or along a σ_{CH2} path, where the carbene p orbital is aligned with a σ_{CH2} fragment orbital.

1 since they possess both an empty p orbital and a lone pair of electrons. Thus, we suggest an idealized approach to either the doubly occupied π_{CH2} hydrocarbon fragment **3a** or the doubly occupied σ_{CH2} fragment **3b** along the axis of the empty p orbital of carbene **4** to arrive at transition state **5** (Figure 1). Of primary importance to the proposed model is that the hydrogen migrates to the larger lobe of the lone pair of electrons on the methylene carbon. In this orientation the migrating hydrogen (H_1) can readily undergo a concomitant 1,2-hydrogen shift to the adjacent pair of electrons on carbon, affording insertion product **6**. Although the trajectory for the incoming electrophile ($^1CH_2$) is along the axis of the atomic p orbital of the σ_{CH2} or π_{CH2} fragment, in the final insertion product the electrophile must be approximately along the C–H bond axis of the initial hydrocarbon. Consequently, after the barrier is crossed, the CHR_1R_2 group must tilt by 35–50°. In addition to the orientation of the carbene in the transition state, we will also address the electronic factors that determine the magnitude of the activation barrier for carbene insertion into a C–H σ bond. Carbenes are highly reactive species that can exist in two electronic states. For the simplest of carbenes, CH_2, the triplet is the ground state, while divalent carbon bearing electronegative substituents with pπ lone pairs has a singlet ground state. The diverse reactivity of a carbene is a direct function of its electronic state. Reactivity trends have been rationalized by a simple valence bond (VB) model based upon reactant and product spin recoupling.[6] In the present study we include a qualitative discussion of the singlet–triplet energy differences (ΔE_{ST}) for carbenes based upon the state correlation diagram (SCD) model described by Shaik and Pross.[7] These data provide a rationale for the relative magnitude of the activation barriers for carbene insertion.

There have been numerous theoretical studies on the concerted pathway for singlet methylene insertion into the hydrogen molecule to afford methane (eq 1).[8] The reaction

$$CH_2(^1A_1) + H_2(^1\Sigma_g^+) \rightarrow CH_4(^1A_1) \qquad (1)$$

is a prototype of a reaction where a Woodward–Hoffmann[9]-allowed and a symmetry-forbidden path can compete. This carbene insertion reaction, which is predicted by theory to proceed by a non-least motion pathway[8c] and to occur without an activation barrier,[8] has also served as a model for singlet methylene insertion into the C–H bonds of saturated hydrocarbons. However, the least motion pathway of reaction 1, maintaining C_{2v} symmetry, is forbidden by orbital symmetry, and configuration interaction (CI) calculations now predict a barrier of 26.7 kcal/mol.[8d] Although the $CH_2 + H_2$ insertion has no barrier, a relatively high level ab initio calculation (MP4/6-311++G(3df,3pd)//MP2/6-311G(2d,2p) predicted a small barrier for SiH_2 insertion into H_2 that is 4.8 kcal/mol above a long-range potential well and 1.7 kcal/mol above reactants.[10a] Schlegel has found a dramatic increase in the barrier heights for insertion into H_2 when methylene or silylene is substituted with either fluorine[11a-e] or chlorine.[11f]

Insertion reactions of methylene into methane[10b] and ethane[10c,d] have been reported at the Hartree–Fock level (barriers of 9.1 and 16.5 kcal/mol, respectively). When third-order Møller–Plesset perturbation theory corrections were included (MP3/6-31G*//HF/3-21G), barriers for CH_2 insertion into methane and ethane were 0 and 0.2 kcal/mol. Experimental data also suggests that the barriers for methylene insertion into hydrocarbons are quite low.[12] Insertion of singlet methylene into the C–H bond of methyl chloride has been studied at the MCSCF//MP2/6-31G* level, and a barrier of 5.4 kcal/mol is predicted.[6] It has been suggested[8b,13] that these reactions occur in two stages, involving an "electrophilic" interaction between the empty p orbital on the methylene carbon and the σ C–H bond and a "nucleophilic" couterpart between the carbene lone pair and the methylene σ^* C–H orbital. Zero barriers were also predicted[10c] for insertion

(6) Bernardi, F.; Bottoni, A.; Robb, M. A. *Mol. Phys.* **1992**, *77*, 51.
(7) (a) Shaik, S. S.; Schlegel, H. B.; Wolfe, S. *Theoretical Aspects of Physical Organic Chemistry*; Codey: New York, 1992. (b) Pross, A.; Shaik, S. S. *Acc. Chem. Res.* **1983**, *16*, 363.
(8) (a) Bauschlicher, C. W., Jr.; Schaefer, H. F., III; Bender, C. F. *J. Am. Chem. Soc.* **1976**, *98*, 1653. (b) Kollmar, H.; Staemmler, V. *Theor. Chim. Acta (Berlin)* **1979**, *51*, 207. (c) Jezioreak, D.; Zurawski, B. *Int. J. Quantum Chem.* **1979**, *26*, 277. (d) Bauschlicher, C. W., Jr.; Haber, K.; Schaefer, H. F., III; Bender, C. F. *J. Am. Chem. Soc.* **1977**, *99*, 3610.
(9) Woodward, R. B.; Hoffmann, R. *The Conservation of Orbital Symmetry*; Verlag Chemie: Weinheim/Bergstr., Germany, 1970.
(10) (a) Gordon, M. S.; Gano, D. R. *J. Am. Chem. Soc.* **1984**, *106*, 5421. (b) Gordon, M. S.; Boatz, J. A.; Gano, D. R.; Friederichs, M. G. *J. Am. Chem. Soc.* **1987**, *109*, 1323. (c) Gano, D. R.; Gordon, M. S.; Boatz, J. A. *J. Am. Chem. Soc.* **1991**, *113*, 6711. (d) Gordon, M. S.; Gano, D. R.; Binkley, J. S.; Frisch, M. J. *J. Am. Chem. Soc.* **1986**, *108*, 2191.
(11) (a) Sosa, C.; Schlegel, H. B. *J. Am. Chem. Soc.* **1984**, *106*, 5847. (b) Schlegel, H. B.; Sosa, C. *J. Phys. Chem.* **1985**, *89*, 537. (c) Francisco, J. S.; Schlegel, H. B. *J. Chem. Phys.* **1988**, *88*, 3736. (d) Gonzales, C.; Schlegel, H. B.; Francisco, J. S. *Mol. Phys.* **1989**, *66*, 859. (e) Ignacio, E. W.; Schlegel, H. B. *J. Phys. Chem.* **1992**, *96*, 1620; 96, 1758. (f) Su, M.-D.; Schlegel, H. B. *J. Phys. Chem.*, submitted for publication.
(12) (a) Jones, M.; Moss, R. A.; *Carbenes*; Wiley: New York, 1972; Vol. 1; 1975; Vol. 2. (b) Kirmse, W. *Carbene Chemistry*; Academic: New York, 1971.
(13) (a) Kollmar, H. *J. Am. Chem. Soc.* **1978**, *100*, 2660. (b) Dobson, R. C.; Hayes, D. M.; Hoffmann, R. *J. Am. Chem. Soc.* **1971**, *93*, 6188.

of SiH_2 into SiH_4. However, SiH_2 insertion into a C–H bond of methane had a predicted activation energy of 22 kcal/mol that compares favorably with an estimated experimental barrier[14] of 17–19 kcal/mol. It was suggested[10c] that the barriers and activation energies correlated with the length of the substrate bond and that steric interactions appear to be a major factor in determining barrier heights. In contrast to the concepts outlined in Figure 1, all of the transition states reported[10] for $^1CH_2$ insertion predicted that the hydrogen would migrate to the opposite face of the methylene lone pair. Migration of a positive hydrogen to the smaller lobe of the nucleophilic carbon appeared to us to be counterintuitive and prompted us to also examine the question of lone pair orientation in the transition state for carbene insertion.

Method of Calculation. Molecular orbital calculations were carried out using the Gaussian 92 program system[15a] utilizing gradient geometry optimization.[15b] The geometries of the reactants and transition structures were first determined at the Hartree–Fock (HF) level of theory with the 3-21G and 6-31G* basis sets. All geometries were then fully optimized using second-order Møller–Plesset perturbation theory (MP2/6-31G*). Relevant energies and barrier heights were computed with the 6-31G* basis set using fourth-order Møller–Plesset perturbation theory (frozen core, MP4SDTQ/6-31G*//MP2/6-31G*). Vibrational frequency calculations at the MP2/6-31G* level were used to characterize all stationary points as either minima (zero imaginary frequencies), first-order transition states (a single imaginary frequency), or second-order saddle points, SOSP (two imaginary frequencies).

Results and Discussion

Singlet Methylene Insertion into Methane. The FMO model suggests that singlet methylene ($^1CH_2$) may approach methane from two unique directions. As illustrated in Figures 1 and 2, the empty p orbital on the methylene carbon may either interact with a filled fragment orbital of π symmetry, as indicated in **7a**, or it may approach a σ_{CH2} orbital, as in **7b**. In an earlier study ab initio calculations predicted that electrophilic oxygen approach to methane in a σ_{CH2} fashion was slightly favored over the π_{CH2} orientation.[4] In preliminary calculations on methylene insertion the two transition states we examined were constrained to C_s symmetry. We found that the σ_{CH2} approach in TS-1, a first-order saddle point, is 0.4 kcal/mol lower in energy than the π_{CH2} orientation, a second-order saddle point SOSP-8 at the HF/6-31G* level (Figure 3 and Table I). In consonance with the FMO model,[4] the σ_{CH2} hydrocarbon fragment approaches the empty 2p orbital on the methylene, affording TS-1. When all of the geometry constraints in SOSP-8 were released, the geometry optimized to TS-1. In this orientation the product ethane is formed in its staggered conformation. We next examined the preferred orientation of the methylene lone pair with respect to the migrating hydrogen. Intuitively, hydrogen migration to the larger lobe of the methylene lone pair should have a lower activation barrier than hydrogen migration to the back side of the methylene carbon. Consistent with this hypothesis TS-2 is 7.3 kcal/mol (HF/6-31G*) higher in energy than SOSP-8 (Figure 3).

Møller–Plesset perturbation theory has been shown to give much better estimates of the barrier heights and transition-state geometries for methylene insertion into C–H bonds.[10] However, all attempts to locate a transition structure for the σ_{CH2} approach in TS-1 or π_{CH2} attack in SOSP-8 at MP2/6-31G* were unsuccessful. Intermediate data for the optimization indicate that insertion by the σ_{CH2} approach is barrierless at the MP2/6-31G* level. We were able to find a first-order saddle point for methylene ($^1CH_2$) insertion into a π_{CH2} orbital where the methylene lone pair is inverted and hydrogen H_1 migrates to the back side of the methylene lone pair (TS-2). The latter TS exhibits a small activation barrier (2.78 kcal/mol), relative to isolated reactants, at the MP4/6-31G*//MP2/6-31G* level, presumably reflecting the less favorable electron density at the methylene carbon (C_1). The MP2 geometry is quite comparable to that calculated at QCISD/6-31G*, but the barrier height for TS-2 is increased to 6.2 kcal/mol. Since hydrogen migration to the larger lobe of the carbene lone pair is more facile, TS-1 would be expected to have a lower barrier than insertion to the opposite face, as shown in TS-2. Multiple pathways have previously been noted for extrusion of SiH_2 from $C_2H_5SiH_3$, affording ethane[11d] and $SiH_2 + SiH_4$.[11e] The transition state for the reverse reaction, corresponding to the insertion of SiH_2 into ethane with hydrogen migration to the larger lobe of the silicon lone pair, was 10.0 kcal/mol (HF/3-21G) lower in energy than the TS where the smaller lobe of the silylene was involved. With this exception, the transition structures reported earlier for $^1CH_2$ and $^1SiH_2$ insertion into the C–H bond of alkanes have all involved the inverted configuration of the divalent carbon or silicon center.

In general, the stereochemistry of CH_2 insertion is adequately described by the HF method, but the barriers are 10–15 kcal/mol too high and the C–C bond distances are 0.2–0.4 Å too short. Since there are significant qualitative differences between the Hartree–Fock and MP2 descriptions of methylene insertion, it is important to check these findings at a higher level of theory. The QCISD approach provides a better description of electron correlation than MP2. Despite the long C–C bond distance (2.86 Å) in the reactant cluster (Figure 3), the methylene fragment ($^1CH_2$) is poised to insert in a σ_{CH2} fashion and the C_2–H_1 bond in the methane fragment is slightly elongated (1.102 Å). Thus, the reaction trajectory for C–H insertion suggested by this FMO model appears to be set in motion in the reactant cluster (see also reactant cluster **9** in Figure 5). The QCISD/6-31G*-optimized transition state is significantly earlier, as evidenced by a relatively long C–C bond (2.503 Å). The barrier at the QCISD/6-31G*

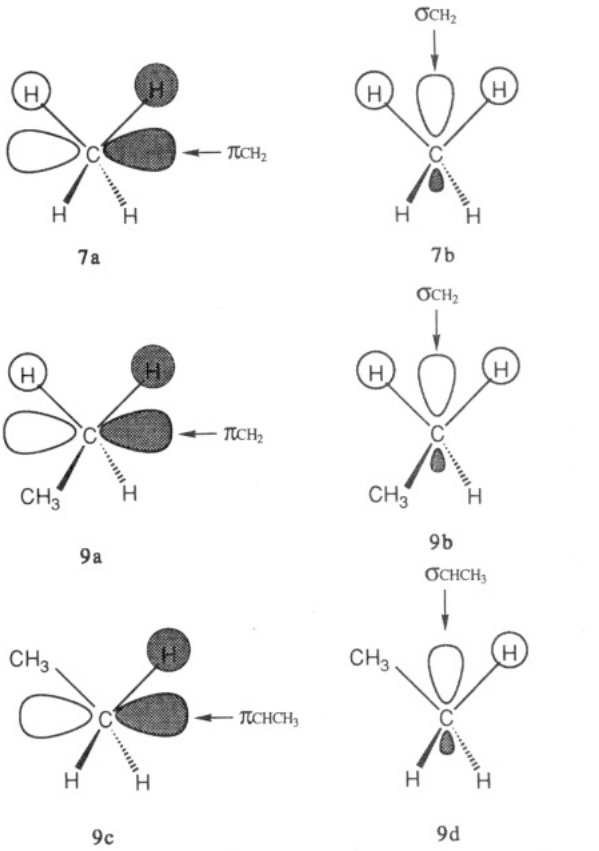

Figure 2. Orientation of singlet carbene attack on the filled fragment orbitals of methane and ethane.

(14) Davidson, I. M. T.; Lawrence, F. T.; Ostah, N. A. *J. Chem. Soc., Chem. Commun.* **1980**, *659*.

(15) (a) Frisch, M. J.; Trucks, G. W.; Head-Gordon, M.; Gill, P. M. W.; Wong, M. W.; Foresman, J. B.; Johnson, B. G.; Schlegel, H. B.; Robb, M. A.; Replogle, E. S.; Gomperts, R.; Andres, J. L.; Raghavachari, K.; Binkley, J. S.; Gonzalez, C.; Martin, R. L.; Fox, D. J.; Defrees, D. J.; Baker, J.; Stewart, J. J. P.; Pople, J. A. *GAUSSIAN 92*; Gaussian, Inc.: Pittsburgh, PA, 1992. (b) Schlegel, H. B. *J. Comput. Chem.* **1982**, *3*, 214.

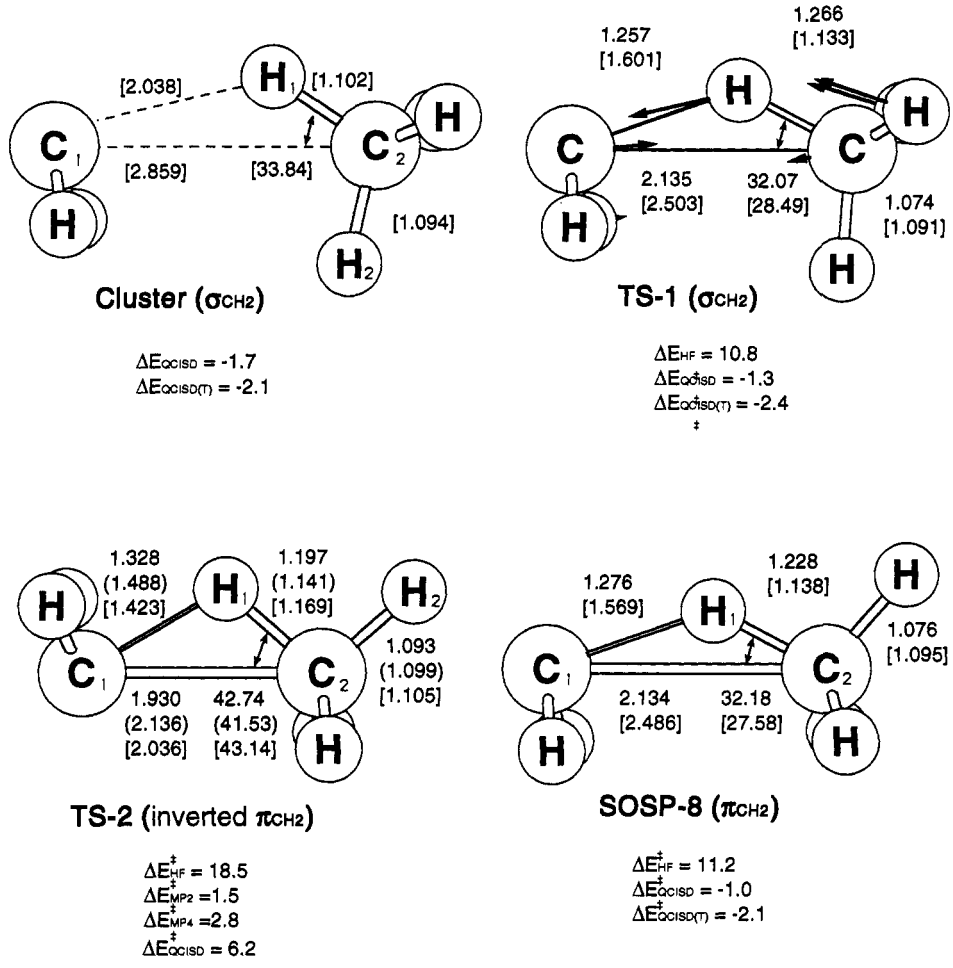

Figure 3. Cluster, transition states, and second-order saddle points for singlet methylene insertion into methane. Geometries have been optimized at HF/6-31G* (no parentheses), MP2/6-31G* (parentheses), and QCISD/6-31G* (brackets); bond lengths are given in angstroms, angles in degrees. Barriers relative to reactants (in kcal/mol) have been calculated at HF/6-31G*, MP2/6-31G*, MP4/6-31G*//MP2/6-31G*, QCISD/6-31G*, and QCISD(T)/6-31G*//QCISD/6-31G*. The transition vector shown for TS-1 was computed at QCISD/6-31G*. The QCISD/6-31G* barriers calculated from the reactant cluster without and with ZPE are 0.40 and 1.06 kcal/mol, respectively.

Table I. Total Energies and Barriers for Methylene Insertion into Methane

	total energies (au)			barriers (kcal/mol)		
level of theory	TS-1 (σ_{CH_2})	SOSP-8 (τ_{CH_2})	TS-2 (inverted π_{CH_2})	TS-1 (σ_{CH_2})	SOSP-8 (π_{CH_2})	TS-2 (inverted π_{CH_2})
HF/6-31G*	−79.050 30	−79.049 70	−79.038 08	10.8	11.2	18.5
MP2/6-31G*	*a*	*a*	−79.308 74	*a*	*a*	1.45
MP4/6-31G*//MP2/6-31G*	*a*	*a*	−79.344 16	*a*	*a*	2.8
QCISD/6-31G*	−79.351 31	−79.350 77		−1.3	−1.0	
QCISD(T)/6-31G*//QCISD/6-31G*	−79.358 14	−79.357 70		−2.4	−2.1	
QCISD(T)/6-311+G(2df,p)//QCISD(T)/6-31G*	−79.486 45			−4.2[b]		

[a] No transition state could be found; insertion proceeds without a barrier. [b] The barrier relative to isolated reactants. At this level TS-1 is 1.77 kcal/mol lower in energy than its reactant cluster at the same level of theory.

level is −1.34 kcal/mol for σ_{CH_2}-oriented singlet methylene insertion into methane (TS-1 in Figure 3 and Table I). Although the negative barrier could be due to basis set superposition error, it is most likely a consequence of a small degree of C–C bonding. The transition state is only 0.4 kcal/mol above the reactant cluster, the methane portion of the transition structure is 1.15 kcal/mol higher in energy than ground-state methane, and the methylene fragment was essentially unperturbed in the transition state, being only 0.02 kcal/mol higher in energy than ground-state $^1CH_2$. Despite the extremely weak interaction, TS-1 is a first-order saddle point, as determined by a numerical frequency calculation at the QCISD/6-31G* level. The normal mode associated with the single imaginary frequency (see Figure 3) is consistent with this insertion process, primarily C–C bond formation and H transfer. Inclusion of the triple excitation at this level (QCISD(T)/6-31G*//QCISD/6-31G*) affords a barrier for TS-1 of −2.36 kcal/mol. When the barrier height is measured from the reactant cluster (QCISD/6-31G*) with zero-point energy (ZPE), the barrier is 1.06 kcal/mol. However, when the triple excitations are included, the barrier is −0.28 kcal/mol, but with ZPE the barrier is 1.04 kcal/mol. We were unable to find a transition state at the QCISD(T)/6-31G* or QCISD/6-311G* levels. Activation barriers calculated at these levels on the QCISD/6-31G* geometries for the cluster and TS-1 were −0.28 and −1.48 kcal/mol, respectively (without ZPE). When the activation barrier was computed at QCISD(T)/6-311+G(2df,p) on the QCISD/6-31G* geometry, TS-1 was 1.77 kcal/mol lower in energy than the reactant cluster and the overall energy difference between isolated reactants and TS-1 was −4.2 kcal/mol. We conclude from these data that the insertion process is barrierless.

Methylene Insertion into Ethane. There are six distinguishable orientations for insertion into a σ_{C-H} bond of ethane where the

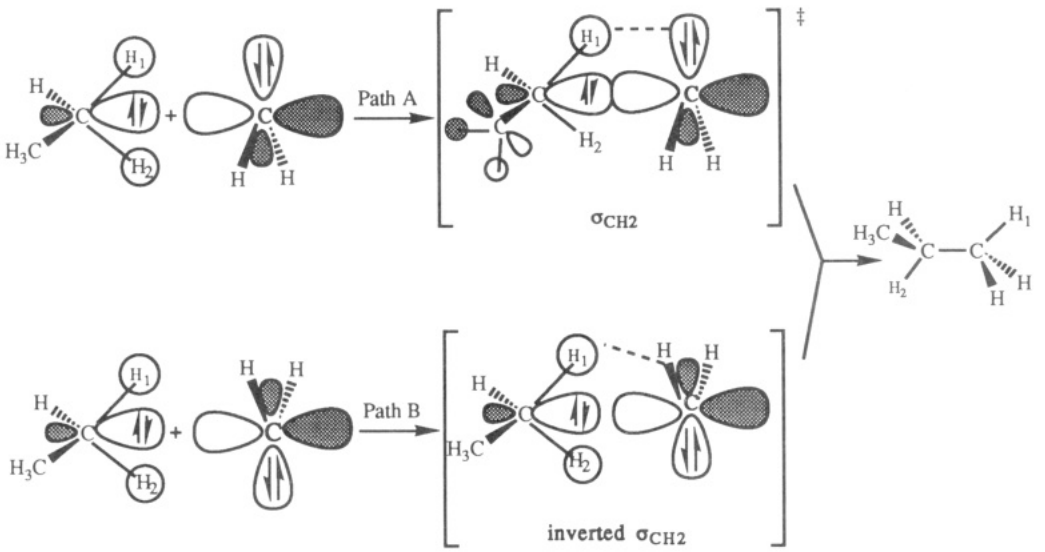

Figure 4. Methylene insertion into ethane via the σ_{CH2} approach (path A) and the inverted σ_{CH2} approach (path B).

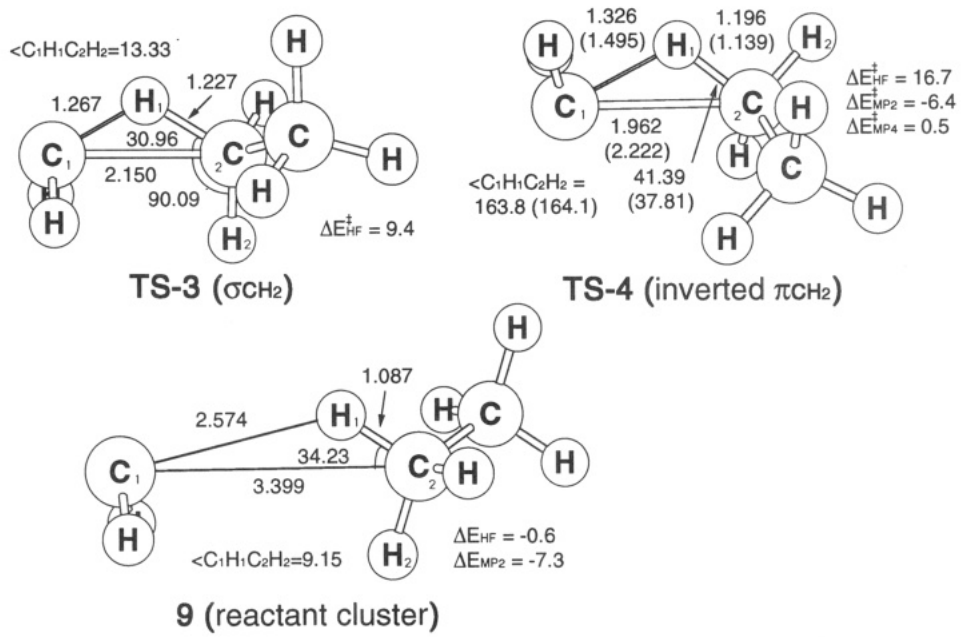

Figure 5. Transition states and second-order saddle points for singlet methylene insertion into ethane. Geometries have been optimized at HF/6-31G* (no parentheses) and MP2/6-31G* (parentheses); bond lengths are given in angstroms, angles in degrees. Barriers relative to reactants (in kcal/mol) have been calculated at HF/6-31G*, MP2/6-31G*, and MP4/6-31G*//MP2/6-31G*.

hydrogen migrates to the more nucleophilic face of singlet methylene. There are two equivalent (mirror image) approaches of $^1CH_2$ to the π_{CH2} orbital in ethane, as illustrated in **9a**, and two mirror image orientations for attack in a σ_{CH2} fashion (**9b**, Figure 2). Interchanging a hydrogen and methyl group affords π_{CHCH3} and σ_{CHCH3} orbitals. Hence, the two additional potential transition structures involve interaction of the electrophilic carbene 2p orbital along the axis of the π_{CHCH3} orbital (**9c**) and between the methyl group and hydrogen (σ_{CHCH3}), as in **9d**.

The σ_{CH2} and π_{CH2} approaches of methylene insertion into ethane are very similar to the insertions into methane. At the Hartree–Fock level, the σ_{CH2} approach (path A, Figure 4) leads to a transition state, TS-3 (Figure 5), but the inverted σ_{CH2} approach (path B) yields a second-order saddle point. The π_{CH2} attack also gives a second-order saddle point, but the inverted π_{CH2} attack involves a first-order saddle point, TS-4. By contrast, all of the σ_{CHCH3} and π_{CHCH3} routes to insertion lead to second-order saddle points.

Despite numerous attempts, we could not locate a transition state for $^1CH_2$ insertion into ethane for the electronically preferred σ_{CH2} approach (path A) at the MP2/6-31G* level. Reaction coordinate following established that $^1CH_2$ insertion by path A as shown in TS-3 occurred without a barrier at the MP2/6-31G* level of theory (Table II). We did find relatively small activation barriers of less than 1 kcal/mol for hydrogen transfer in the inverted configuration (path B) for the π_{CH2} (TS-4) approach to ethane. We suspect that we were only able to find a transition state for path B because of the less favorable interaction of the inverted lone pair of electrons with the migrating hydrogen. The more hindered σ_{CHCH3} orientation had an MP4SDTQ/6-31G*//MP2/6-31G* barrier of 9.4 kcal/mol. From these data we conclude that singlet methylene will preferentially approach a simple hydrocarbon in a σ_{CH2} fashion, that the hydrogen will migrate to the larger lobe of the attacking carbene, and that insertion will take place with little or no activation barrier.

Singlet Vinylidene Insertion into the C–H Bonds of Methane and Ethane. Although the energy differences between the σ_{CH2} and π_{CH2} approaches to methane and ethane are relatively small, in each case the orientation of the lone pair and empty 2p orbital on the methylene carbon was consistent with the basic concepts

Table II. Total Energies (au) and Barriers (kcal/mol) for Methylene Insertion into Ethane

compd	orientation	HF/6-31G*	MP2/6-31G*	MP4SDTQ/6-31G*// HF/6-31G*	MP4SDTQ/6-31G*// MP2/6-31G*
			total energies		
methylene		−38.872 37	−38.974 01	−38.993 37	−38.993 79
ethane		−79.228 76	−79.494 74	−79.532 34	−79.532 81
TS-3	σ_{CH2}	−118.086 22		−118.543 27	−118.525 38
TS-4	π_{CH2}	−118.074 50	−118.479 02	−118.527 83	−118.525 79[a]
14		−118.102 09[d]	−118.480 37[d]	−118.528 44	
			Barriers		
TS-3	σ_{CH2}	9.36	−6.44 (0.85)[c]	−11.02 (−9.31)[e]	
TS-4	π_{CH2}	16.72	−4.45 (2.84)[c]	−1.33 (0.38)[e]	0.51[a,b]
14		−0.60	−7.29	−1.71	

[a] Geometry was constrained to a σ_{CH2} orientation. The total energy was −118.536 40 when the constraint was removed. [b] The lone pair of electrons on the methylene has the inverted configuration (path B). [c] Activation barriers in parentheses have been calculated relative to reactant cluster 9 based upon a MP2/6-31G*//HF/6-31G* energy. [d] At the MP2/6-31G*//HF/6-31G* level. [e] Barriers relative to reactant cluster 9 based upon a MP2/6-31G*//HF/6-31G* energy.

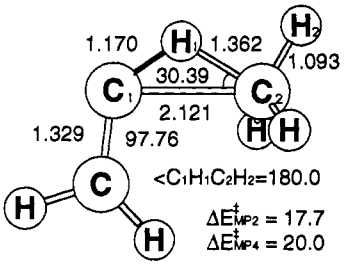

TS-5 (π_{CH2})

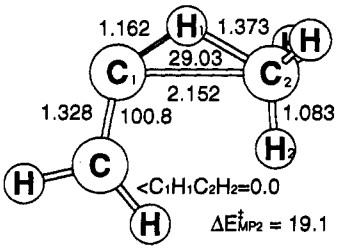

SOSP-10 (σ_{CH2})

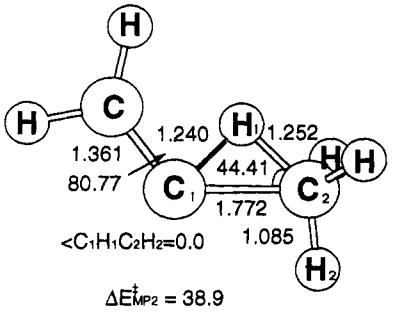

SOSP-11 (inverted σ_{CH2})

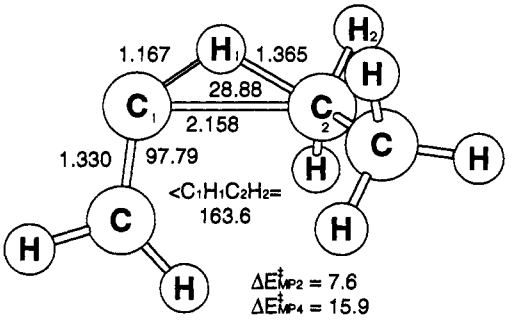

TS-6 (π_{CH2})

Figure 6. Transition states and second-order saddle points for vinylidene insertion into the C–H bond in methane and ethane. Geometries have been optimized at MP2/6-31G*; bond lengths are given in angstroms, angles in degrees. Barriers relative to reactants (in kcal/mol) have been calculated at MP2/6-31G* and MP4/6-31G*//MP2/6-31G*. Total energies of TS-5, SOSP-10, SOSP-11, and TS-6 at MP2/6-31G* are −117.303 18, −117.301 00, −117.269 43, and −156.477 01 au, respectively; total energies of TS-5 and TS-6 at MP4/6-31G*//MP2/6-31G* are −117.344 70 and −156.529 15 au, respectively.

outlined in the FMO model. Although vinylidene is a short-lived carbene that is principally of theoretical interest, it presents itself as an excellent model to test steric requirements for insertion since it has an empty 2p orbital that lies in the same plane as its trigonally hybridized adjacent methylene group. In this case we found that the π_{CH2} approach to methane was slightly favored and the MP4//MP2/6-31G* activation barrier for TS-5 is 20.0 kcal/mol. The σ_{CH2} approach is a second-order saddle point (SOSP-10) that is 1.4 kcal/mol higher in energy (Figure 6). The orientation of the lone pair on the sp carbon is also very important since SOSP-11, which is comparable to path B, is 19.8 kcal/mol higher in energy than SOSP-10. The MP4SDTQ/6-31G*// MP2/6-31G* activation barrier (15.9 kcal/mol) for insertion into ethane (TS-6) is 4.1 kcal/mol lower than that for methane insertion, reflecting the stabilizing influence of the filled π_{CH2} orbitals on adjacent methyl groups.[4] Steric interactions between the methyl and methylene groups cause a deviation from the idealized π_{CH2} approach, and the $C_1H_1C_2H_4$ dihedral angle is 163.6° in TS-6. Although we did not make a thorough search for other possible reaction trajectories for vinylidene insertion, in general we have found that there is only one first-order saddle point with the proper orientation of the carbene lone pair and we do not necessarily seek other approaches that are of higher order. However, as noted below, transition structures for hydrogen migration to either face of the carbene (Figure 4) can be a first-order process.

Insertion Reactions of Silylene, Fluoro Carbenes, and Methyl Carbenes. We next reexamined the transition structures for silylene insertion into ethane at the MP2/6-31G* level. Both pathways (Figure 4) for hydrogen migration had previously been reported at the HF level.[11d] Our objective here is to establish the reaction trajectory. Within the context of this FMO model, singlet SiH_2 insertion into ethane proceeds by a σ_{CH2} pathway (TS-7, Figure 7) with a barrier of 22.3 kcal/mol. Although the π_{CH2} insertion pathway with the inverted silylene configuration (path B) is also a first-order saddle point (TS-8), it lies 7.8 kcal/mol

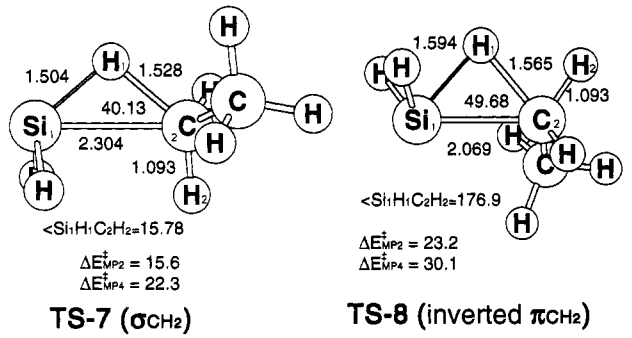

Figure 7. Transition states for silylene insertion into the C–H bond of ethane. Geometries have been optimized at MP2/6-31G*; bond lengths are given in angstroms, angles in degrees. Barriers relative to reactants (in kcal/mol) have been calculated at MP2/6-31G* and MP4/6-31G*//MP2/6-31G*. Total energies of TS-7 and TS-8 are −369.547 10 and −369.534 96 au, respectively, at MP2/6-31G* and −369.587 43 and −369.575 15 au, respectively, at MP4/6-31G*//MP2/6-31G*.

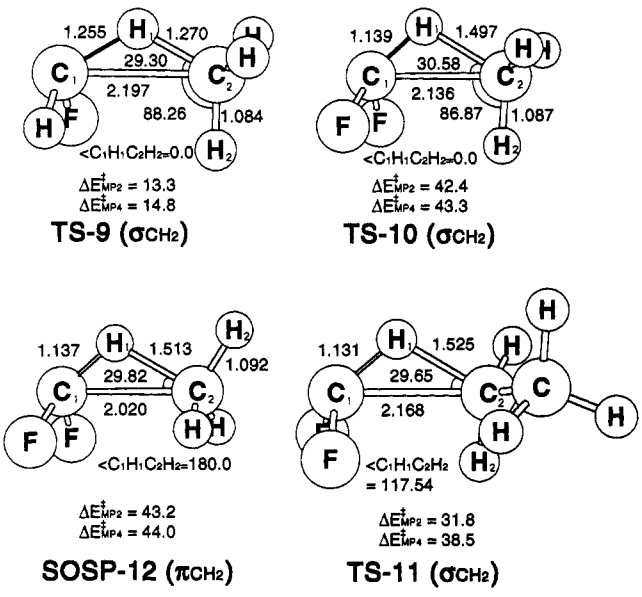

Figure 8. Transition states and second-order saddle points for fluoro carbene and difluoro carbene insertion into the C–H bond of methane and ethane. Geometries have been optimized at MP2/6-31G*; bond lengths are given in angstroms, angles in degrees. Barriers relative to reactants (in kcal/mol) have been calculated at MP2/6-31G*, MP4/6-31G*//MP2/6-31G*, and QCISD(T)//MP2/6-31G*. Total energies of TS-9, TS-10, SOSP-12, and TS-11 are −178.351 88, −277.389 99, −277.388 64, and −316.564 50 au, respectively, at MP2/6-31G* and −178.387 58, −277.425 89, −277.424 85, and −316.611 49 au, respectively, at MP4/6-31G*//MP2/6-31G*. The total energies for CH_4, CHF, and TS-9 at QCISD(T)//MP2/6-31G* are −40.355 96, −138.056 99, and −178.389 16 au.

higher in energy than TS-7. This overall insertion process mirrors the $^1CH_2$ insertion process, except it exhibits a much higher activation barrier.

We also felt that it would be prudent to examine the insertion pathways for halo-substituted carbenes and methyl-substituted carbenes to see if they are consistent with the FMO model. Monofluoro carbene (^{1}CHF) approaches methane in the σ_{CH_2} fashion, and the insertion reaction (TS-9, Figure 8) is associated with a fairly large activation barrier (14.8 kcal/mol). When the barrier was computed at the QCISD(T)/6-31G* level on the MP2 geometry, it was essentially unchanged (14.9 kcal/mol). We found the σ_{CH_2} orientation for CF_2 insertion into both methane and ethane to be slightly preferred to the π_{CH_2} approach. The σ_{CH_2} approach (TS-10) is a first-order saddle point that is 0.7 kcal/mol lower in energy than SOSP-12 (Figure 8). However, it should also be emphasized that the π_{CH_2} approach in **12** affords

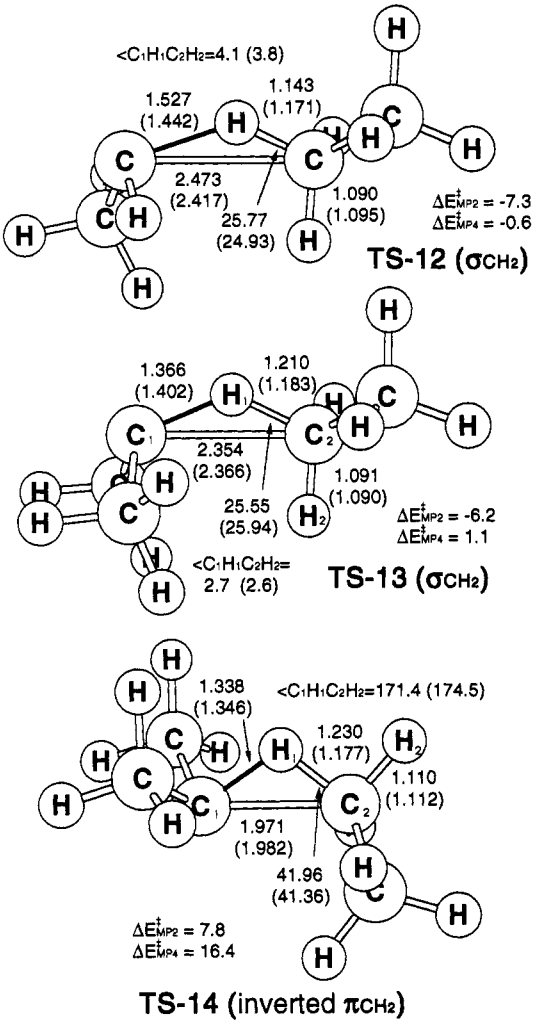

Figure 9. Transition states for methyl carbene and dimethyl carbene insertion into the C–H bond of ethane. Geometries have been optimized at MP2/6-31G*; bond lengths are given in angstroms, angles in degrees. Barriers relative to reactants (in kcal/mol) have been calculated at MP2/6-31G* and MP4/6-31G*//MP2/6-31G*. Total energies of TS-12, TS-13 and TS-14 are −157.666 94, −196.847 34, and −196.825 14 au, respectively, at MP2/6-31G* and −157.724 89, −196.914 99, and −196.890 58 au, respectively, at MP4/6-31G*//MP2/6-31G*.

an eclipsed conformation upon insertion. The activation barrier for singlet CF_2 insertion into ethane is 38.5 kcal/mol. This barrier (TS-11) is 4.8 kcal/mol lower than the CF_2 barrier for insertion into methane, in consonance with the relative barriers noted for the other insertion reactions.

Whereas the primary effect of fluorine substitution is on the electronic structure of the carbene, methyl substitution also exerts a steric influence. Methyl carbene ($^1CHCH_3$) approaches ethane in a σ_{CH_2} orientation (TS-12, Figure 9) and has a small negative barrier. Dimethyl carbene ($^1C(CH_3)_2$) also proceeds in a σ_{CH_2} fashion but with a small positive barrier (1.1 kcal/mol) (TS-13, Figure 9). In the π_{CH_2} approach, dimethyl carbene prefers the inverted over the regular orientation because of steric interactions (TS-14).

It is worthy of note that the magnitude of the activation barriers for hydrocarbon insertion that we have examined so far depends more strongly on electronic factors than on steric interactions. For example, the activation barriers for methyl and dimethyl carbene inserting into ethane are −0.6 and 1.1 kcal/mol, but those for vinylidene and difluoro carbene insertion into methane are 20.0 and 43.3 kcal/mol, respectively. The barrier for silylene insertion also increases markedly with halogen substitution.[11e,f] The TS for CF_2 insertion (TS-11) comes much later along the reaction coordinate than that for CH_2 insertion (TS-4), as reflected

Table III. Singlet–Triplet Energy Gaps (ΔE_{ST}), HOMO and LUMO Energies (au), and Barriers (kcal/mol) for Insertion into Methane and Ethane

					activation barriers					
					HF/6-31G*		MP2/6-31G*		MP4//MP2/6-31G*	
reactant	ΔE_{ST}[a]	HOMO[a]	LUMO[a]	ΔE_{HO-LU}[a]	CH_4	C_2H_6	CH_4	C_2H_6	CH_4	C_2H_6
methane		−0.5446	0.2559	0.8005						
ethane		−0.4858	0.2418	0.7276						
CH_2	−22.1	−0.3867	0.0724	0.4591	10.8	9.4			2.8[b]	0.51[b]
$HCCH_3$	−15.3	−0.3522	0.0948	0.4770				−7.3		−0.56
$C(CH_3)_2$	−9.98	−0.3253	0.1039	0.4292				−6.2		1.1
CHF	7.69	−0.4028	0.0898	0.4926	30.5		13.3		14.8	
SiH_2	12.9	−0.3358	0.0082	0.3440			15.6		22.3	
$H_2C{=}C$	38.5	−0.4023	0.0857	0.4880	41.9		17.7	7.6	20.0	15.9
CF_2	51.3[c]	−0.4718	0.1015	0.5733	63.7		42.4	31.8	43.3	38.5

[a] All energies given were calculated at MP2/6-31G* unless specified otherwise. [b] Hydrogen migration to the smaller lobe of the carbene lone pair (path B). [c] The singlet–triplet energy gap is 53.2 at QCISD/6-311G** and 55.0 at the QCISD(T)/6-31G**//QCISD/6-31G** level.

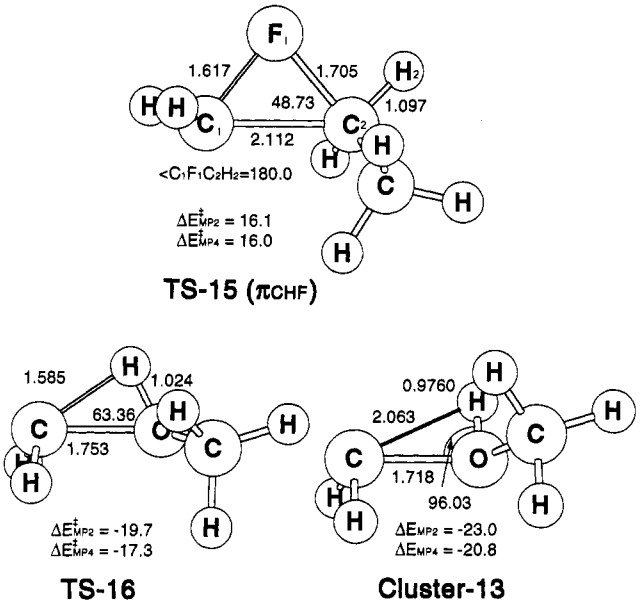

Figure 10. Transition states and reactant cluster for singlet methylene insertion into the C–F bond of ethyl fluoride and into the O–H bond of methanol. Geometries have been optimized at MP2/6-31G*; bond lengths are given in angstroms, angles in degrees. Barriers relative to reactants (in kcal/mol) have been calculated at Mp2/6-31G* and MP4/6-31G*//MP2/6-31G*. Total energies of TS-15, TS-16, and cluster-13 are −217.468 63, −154.358 71, and −154.363 91 au, respectively, at MP2/6-31G* and −217.517 90, −154.395 20, and −154.400 73 au, respectively, at MP4/6-31G*//MP2/6-31G*.

in the relative C_2–H_1 bond distances of 1.525 and 1.139 Å and the charges on H_1 of 0.31 and 0.16, respectively, whereas the methyl and dimethyl carbene transition structures are very similar to methylene insertion.

Carbene Insertion into C–F and O–H Bonds. Electronic factors associated with the lone pairs of electrons on the substrate can also influence the pathway for methylene insertion. For example, insertion of $^1CH_2$ into the C–F bond of ethyl fluoride follows a reaction pathway comparable to path B (Figure 10). The lone pairs of electrons on the fluorine interact with the empty 2p orbital on the methylene carbon. The four-electron repulsion is minimized when the carbene lone pair is directed away from the migrating fluorine (TS-15). This insertion reaction has a relatively high activation energy ($\Delta E^{\ddagger}$ = 16.0 kcal/mol), reflecting the repulsive nature of the two reactants. Insertion of SiH_2 into the Si–F bond of H_3SiF also proceeds by path B.[11b] However, $^1CH_2$ insertion into an O–H bond of methanol follows path A. The higher lying oxygen lone pair appears to mix with the electrophilic carbon 2p orbital and produces a reactant cluster **13** that lies 20.8 kcal/mol below the reactants. Hydrogen migration proceeds in a manner analogous to that for hydrocarbon insertion (TS-16) with a transition state 3.5 kcal/mol above reactant cluster **13**.

The Origin of the Barrier for Carbene Insertion. It appears that an increase in the size of the basis set and the level of theory results in the disappearance of an activation barrier for insertion of $^1CH_2$ into the hydrogen molecule.[10d] In a similar fashion, the barrier for $^1CH_2$ insertion into methane and ethane exhibits 0 or negative values[10a–c] at the MP4//MP2/6-31G* level. However, SiH_2 insertion into C–H bonds is associated with barriers in the 10–17 kcal/mol range.[14] The increase in barrier heights for SiH_2 insertion has been attributed to steric interactions[10c] and to simple perturbational molecular orbital (PMO) arguments.[11a] The overall process for $^1CH_2$ insertion into a saturated hydrocarbon involves the breaking and making of a σ_{C-H} bond and the exothermicity attending the formation of a new carbon–carbon single bond. Since this is a highly exothermic reaction, conventional wisdom has predicted an early transition state and no activation barrier. A perusal of the various transition structures for $^1CH_2$ insertion suggests that the C–C bond distance in the transition state is 2.0–2.5 Å. Upon closer examination of the transition structure for $^1CH_2$ insertion, it became evident that *the C–C σ bond is formed after the barrier is crossed.* While the FMO model provides a reaction trajectory, consummation of the interaction of the electrophilic 2p carbon orbital and the filled σ_{CH2} or π_{CH2} hydrocarbon fragment orbital is not realized until after the barrier is crossed. If this is indeed true and $^1CH_2$ insertion into a hydrocarbon involves perturbation of the C–H_1 bond, then in the absence of electronic effects, this overall reaction should exhibit a small but discernible activation barrier.

We have examined a broad range of insertion reactions, and it is evident that neither steric effects nor FMO arguments based upon HOMO–LUMO energy gaps correlate well with the increase in insertion barriers. However, an increase in the energy difference between the singlet and triplet state (ΔE_{ST}) of the carbene or silylene is associated with a general increase in the activation energy for insertion at all levels of theory (Table III). For example, at the MP2/6-31G* level the methylene $^3B_1$ triplet state lies 22.1 kcal/mol below the $^1A_1$ singlet state. The methyl ($HCCH_3$) and dimethyl carbene ($C(CH_3)_2$) ΔE_{ST}'s are −15.3 and −9.98 kcal/mol, respectively. Consequently, if this hypothesis has merit, then one could predict that a modest increase in the barrier for insertion should be observed as the ΔE_{ST} increases. Although no TS could be found for $^1CH_2$ insertion into ethane by path A, the MP4//MP2/6-31G* barriers for $^1CHCH_3$ and $^1C(CH_3)_2$ insertion into ethane are −0.56 and +1.1 kcal/mol, respectively (Figure 9). This series also demonstrates an interesting steric phenomenon since both methyl (TS-12) and dimethyl carbene (TS-13) insert by path A when the approach is σ_{CH2} and the product has a staggered conformation. However, when insertion of the more hindered dimethyl carbene proceeds in a π_{CH2} fashion, steric repulsion between the methyl groups induces an inversion of the carbene and path B is preferred (TS-14). The activation

Table IV. Calculated Singlet–Triplet ($^1A_1$–$^3B_1$) Energy Gap for Methylene (kcal/mol)

level of theory	ΔE_{ST}[a]	methane[e]	ethane[e]
HF/6-31G*	−30.8	10.8	9.36
HF/6-31G**	−29.2		
MP2/6-31G*	−22.1	−6.44 (9.85)	
MP4/6-31G*	−17.2	2.8[f]	0.51[f]
MP4/6-311G**	−14.2		
QCISD/6-31G*	−16.0	−1.3[g]	
QCISD(T)/6-31G*	−15.3		
QCISD/6-311G**	−13.3		
QCISD(T)/6-311G**	−12.5		
full CI(DZP)[b]	−11.97		
SOCI+Q[c] [5s4p3d2f1g/4s3p2d]	−9.07		
experimental[d]	−9.02		

[a] Energy of the triplet state ($^3CH_2$) minus energy of the singlet state ($^1CH_2$) fully optimized with the level of theory indicated. [b] See ref 16c. [c] See refs 16a,b. [d] See ref 17. [e] Activation barriers for the singlet methylene insertion at the level indicated. [f] Using the MP2/6-31G* geometry. [g] Without ZPE.

barrier for TS-14 increases to 16.4 kcal/mol. The migration of H_1 in the electronically disfavored orientation should account for about 7 kcal/mol of the increase in the barrier.

It is possible that an increase in steric interactions rather than ΔE_{ST} is partially responsible for the increase in activation energy in the methyl-substituted carbenes. An alternative approach to separating the effect of ΔE_{ST} and steric interactions on the insertion barrier is to hold the carbene constant and to probe the effect of ΔE_{ST} by varying the level of theory. The singlet-triplet energy gap for methylene has been well studied. Configuration interaction calculations (SOCI+Q)[16] with a large basis set (Table IV) predict a ΔE_{ST} of −9.07 kcal/mol, in excellent agreement with experiment (−9.02).[17] At the Hartree–Fock level ΔE_{ST} is predicted to be −30.8 kcal/mol. However, we calculate a high positive barrier for hydrocarbon insertion that vanishes when third- or fourth-order Møller–Plesset electron correlation is included. The ΔE_{ST} that we calculate for $CHCH_3$ at the MP2/6-31G* level (−15.3 kcal/mol) is also too large since the predicted ΔE_{ST} is −6.1 kcal/mol at the CISD+DVD/TZ+2p+f//CISD/DZP level.[16a] Inspection of the calculated singlet–triplet energy gaps for methylene at the various levels of theory that we have used shows that ΔE_{ST} is approximately reduced by one-half at the QCISD/6-31G* level relative to Hartree–Fock. These data are consistent with the above contention, based upon the extent of bond breaking in the TS, that the insertion of singlet methylene into the C–H bond of a saturated hydrocarbon should proceed with a small nonzero barrier. The singlet state of methylene is higher in energy than the triplet, and the energy gap between $^1A_1$ and $^3B_1$ methylene is low relative to that same energy gap for CF_2 where the singlet is the ground state. For example, at the QCISD(T)/6-311G** level ΔE_{ST} for CH_2 is −12.5 kcal/mol and for CF_2 the singlet is predicted to be 55.0 kcal/mol lower in energy (QCISD(T)/6-31G**//QCISD/6-31G**) than the triplet, in excellent agreement with experiment (56.6 kcal/mol).[18] Consequently, one can qualitatively predict that methylene insertions on the singlet surface will have a lower barrier for those divalent carbon species that have triplet ground states; barriers for carbene insertion where the singlet is the ground state will be relatively high. For substituted carbenes, with the exception of vinylidene, there is a very good correlation between ΔE_{ST} calculated at the MP2/6-31G* level and the activation barriers for insertion into methane and ethane (Figure 11).

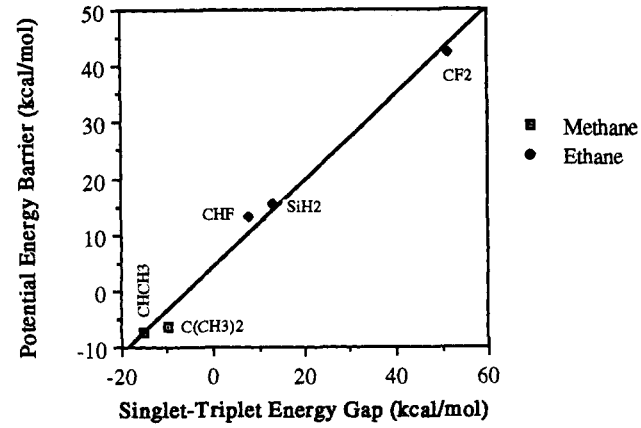

Figure 11. Correlation between the singlet–triplet energy gap of the substituted carbenes and the potential energy barriers for insertion into methane and ethane.

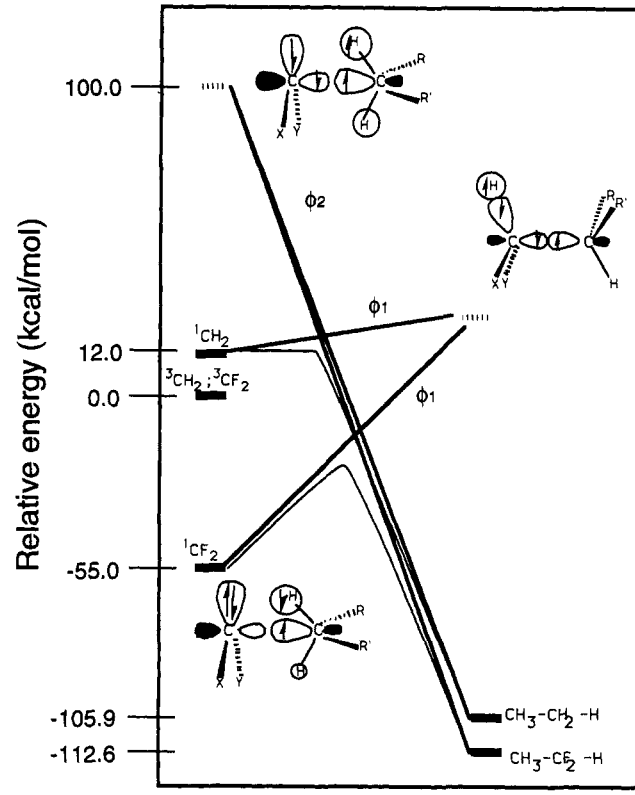

Figure 12. State correlation diagram for carbene insertion into C–H bonds. The energy of the triplet state of the carbene is chosen as 0. The ΔE_{ST}'s are calculated at QCISD(T)/6-311G**. The upper anchor state for the reactants is the singlet coupling between the carbene triplet and the C–H bond triplet; the upper product anchor state is the singlet coupling between a C–C triplet and a C–H triplet (the energies of the upper anchor states are rough approximations).

The conventional PMO analysis involving HOMO–LUMO interactions of both closed-shell reactants does provide an explanation for the difference in activation barriers for CH_2 and CF_2 insertion.[11a] This type of reaction involving a reactant that has two state configurations that can interact with a hydrocarbon can also be conveniently explained by the valence bond state correlation model of Pross and Shaik.[7] An explanation for the surprising differences in activation energy for insertion reactions of methylene and difluoro carbene can be readily displayed in a state correlation diagram (Figure 12). Employing a simple two-configuration interaction for the singlet surface, the reactant ground-state configuration ϕ_1 (^1A–$^1\sigma$) ends up as an excited configuration. The excited configuration of the reactants ϕ_2 (^3B–$^3\sigma^*$) correlates with the ground state of the products. There are

(16) (a) Gallo, M. M.; Schaefer, H. F., III. *J. Phys. Chem.* **1992**, *96*, 1515. (b) Bauschlicher, C. W. Jr.; Langhoff, S. R.; Taylor, P. R. *J. Chem. Phys.* **1987**, *87*, 387. (c) Bauschlicher, C. W., Jr.; Taylor, P. R. *Ibid.* **1986**, *85*, 6510.

(17) (a) Leopold, D. G.; Murray, K. K.; Miller, A. E. S.; Lineberger, W. C. *J. Chem. Phys.* **1985**, *83*, 4849. (b) Bunker, P. R.; Sears, T. *J. Ibid.* **1985**, *83*, 4866. (c) Marshall, M. D.; McKeller, A. R. W. *Ibid.* **1986**, *85*, 3716. (d) Bunker, P. R.; Jensen, P.; Kraemer, W. P.; Beardsworth, R. *Ibid.* **1986**, *85*, 3724.

(18) For a recent discussion of singlet–triplet energy separations, see: Russon, N.; Siclia, E.; Toscano, M. *J. Chem. Phys.* **1992**, *97*, 5031.

two intermediate monoexcited configurations ($\phi_3 = {}^3B\text{–}{}^1\sigma$ and $\phi_4 = {}^1A\text{–}{}^3\sigma^*$) that represent excited triplet states that do not mix with the singlet surfaces. The reaction complex at any point on the reaction profile can be described by Ψ, a linear combination of ϕ_1 and ϕ_2. The character of the transition state will reflect the extent of mixing between ϕ_1 and ϕ_2 in the region of the avoided crossing.

In Figure 12 the triplet states of CH_2 and CF_2 are placed at the origin, and the triplet state of a C–H bond is assumed to be ~100 kcal/mol above its ground state. The exothermicity of the $^1CH_2$ insertion reactions into methane at the QCISD/6-31G* level is 117.9 kcal/mol. The exothermicity of $^1CF_2$ insertion into methane is only 57.6 kcal/mol (MP4//MP2/6-31G*). It has been shown that the dominant factor in determining bond energy trends in the ground state of molecules possessing CXY fragments is the singlet–triplet energy splitting of the corresponding carbene.[19] To a first approximation, the differences in the heats of formation between the two insertion products are the singlet–triplet energy gap for CF_2. The excited state of the products that correlates with the ground-state reactants is assumed to be ca. 100–150 kcal/mol above the ground-state products. The barrier arises from the avoided crossing between ϕ_1 and ϕ_2. Because singlet methylene lies above the triplet, ϕ_1 rises relatively little before it crosses ϕ_2, resulting in a very small barrier. On the other hand, singlet difluoro carbene is much more stable than the triplet; thus, ϕ_1 must rise steeply and yields a high barrier as a result of its crossing with ϕ_2. This overall approach is consistent with the spin recoupling VB model used to describe CH_2 insertion into methyl chloride.[6] The state correlation diagram also indicates that the methylene insertion transition state should be significantly earlier than the difluoro carbene transition state. This is in agreement with the optimized structures shown in Figures 3 and 8 (C_2–H_1 = 1.1–1.2 Å for methylene insertion and ca. 1.5 Å for difluoro carbene insertion).

In summary, this FMO model provides a rationale for the reaction trajectory for carbene insertion into a C–H bond. In most instances the electrophilic carbene 2p orbital approaches the doubly occupied σ_{CH2} fragment orbital of the hydrocarbon, affording the insertion product in the lower energy staggered conformation. Vinylidene inserts in a π_{CH2} fashion to avoid a steric interaction of one of its vinyl hydrogens with hydrogen H_2 of the σ_{CH2} fragment. In more complicated systems the approach of the carbene will deviate from the idealized σ and π trajectories and it is recognized that a rotation about the axis of the developing C–C bond of 60° can interconvert σ and π approaches. The primary purpose of this model is to allow predictions of an approximate pathway and to provide an explanation for the orientation of the carbene lone pair in the TS for insertion. Finally, we feel that we have provided a convincing argument that the magnitude of the activation barrier for insertion exhibits an excellent correlation with the singlet–triplet energy gap of the inserting carbene. This observation makes it quite obvious that, in order to calculate accurately the energetics for carbene insertion, the level of theory employed must be sufficiently high to accurately predict the magnitude of ΔE_{ST}.

Acknowledgment. This work was supported in part by the National Science Foundation (CHE 90–20398) and a NATO Collaborative Research Grant (900707) and the CIRIT of the "Generalitat de Catalunya". We are also thankful to the Pittsburgh Supercomputing Center, CRAY Research, and the Ford Motor Company for generous amounts of computer time.

(19) (a) Carter, E. A.; Goddard, W. A., III. *J. Phys. Chem.* **1986**, *90*, 998. (b) Carter, E. A.; Goddard, W. A., III. *J. Phys. Chem.* **1988**, *88*, 1752.